Cretaceous Research 166 (2025) 106014

Contents lists available at ScienceDirect

Cretaceous Research

journal homepage: www.elsevier.com/locate/CretRes

A new gansuid bird (Avialae, Euornithes) from the Lower Cretaceous (Aptian) Jiufotang Formation of Jianchang, western Liaoning, China

Xuri Wang [a, *], Andrea Cau [b, **], Yinuo Wang [c], Martin Kundrát [d], Guili Zhang [e], Yichuan Liu [f], Luis M. Chiappe [g]

[a] Key Laboratory of Stratigraphy and Paleontology of the Ministry of Natural Resources, Institute of Geology, Chinese Academy of Geological Sciences, 26 Baiwanzhuang Road, Beijing 100037, China
[b] Independent, Imbriani St., Parma 43125, Italy
[c] School of Earth Science and Engineering, Shandong University of Science and Technology, 579 Qianwangang Road, Qingdao 266000, China
[d] Evolutionary Biodiversity Research Group, PaleoBioImaging Lab, Center for Interdisciplinary Biosciences, Technology and Innovation Park, Pavol Jozef Šafárik University in Košice, Jesenná 5, Košice 04001, Slovak Republic
[e] Shandong Institute of Geological Survey, Ji'nan 250013, China
[f] China University of Geosciences, Beijing 100083, China
[g] Natural History Museum of Los Angeles County, Los Angeles, CA, USA

ARTICLE INFO

Article history:
Received 21 July 2024
Received in revised form
18 September 2024
Accepted in revised form 18 September 2024
Available online 24 September 2024

Keywords:
Early Cretaceous
Jehol Biota
Western Liaoning
Avialae
Phylogeny
Osteohistology

ABSTRACT

The study of the Cretaceous birds closest to the living euornithine species has mainly focused on the evolutionary patterns leading to the modern group. Yet, the morphological and ecological diversity of the euornithine branches not directly ancestral to the crown-group is probably underestimated. A new euornithine bird, *Shuilingornis angelai* gen. et sp. nov., is erected based on a nearly complete skeletal material from the Early Cretaceous (Aptian) Jehol Biota in western Liaoning, China. The new taxon is similar to the penecontemporary gansuids, yet it differs in the smaller body size and in the retention of plesiomorphic features widespread among non-gansuid euornithines. The osteohistological analysis indicates that *Shuilingornis* gen. nov. represents an early adult stage at the time of death. The phylogenetic analysis robustly supports the referral of *Shuilingornis* gen. nov. to Gansuidae. Except for the controversial *Hollanda*, the gansuids have been uncovered from four Aptian basins deposited under similar paleoclimatic conditions. Gansuid success in the middle part of the Cretaceous demonstrates that the exploration of semi-aquatic ecologies was a consistent euornithine pattern which preceded the later ornithurine radiation.

1. Introduction

During the last 25 years, an extraordinary diversity of fossil birds has been described from the Early Cretaceous Jehol Group of North Eastern China (Wang et al., 2017; Wang et al., 2022b; Wu et al., 2023; Wang et al., 2024; Zhou and Wang, 2024), including a series of lineages not directly related to the living avians, such as Jeholornithidae, Sapeornithidae, Jinguofortisidae, Confuciusornithidae, and Enantiornithes, together with various taxa closer to the crown group (=Aves/Neornithes), which with the latter form the Euornithes (Chiappe et al., 1999; Zhou and Zhang, 2002; Zhou, 2004, 2014; O'Connor et al., 2015; Wang et al., 2020b). The rich fossil record from the Jehol Biota has documented many steps along the evolutionary process leading to the modern avian skeletal plan from the ancestral avialan condition (Cau, 2018), including key innovations in the skull and mandible (e.g., Zheng et al., 2018; Bailleul et al., 2019), in the flight apparatus (e.g., O'Connor et al., 2010; O'Connor and Zhou, 2012), and in the growth pattern (O'Connor et al., 2015). A pivotal phase of the evolutionary trajectory leading to the origin of the modern birds during the mid-Cretaceous is represented by the *Gansus*-like euornithines (e.g., You et al., 2006; Liu et al., 2014; O'Connor et al., 2015; Wang et al., 2020e). These avialans are among the oldest instances of semi-aquatic adaptations along the bird lineage, showing appendicular innovations suggesting a less arboreal

* Corresponding author.
** Corresponding author.
E-mail addresses: 147966459@qq.com (X. Wang), cauand@gmail.com (A. Cau), 2765051543@qq.com (Y. Wang), martin.kundrat@upjs.sk (M. Kundrát), 34670474@qq.com (G. Zhang), 1976570361@qq.com (Y. Liu), lchiappe@nhm.org (L.M. Chiappe).

https://doi.org/10.1016/j.cretres.2024.106014

lifestyle than in other pygostylians, and hindlimb novelties analogous to those of modern aquatic birds (You et al., 2006). The monophyly and inclusiveness of the "gansuid group" are both controversial, with different studies supporting the group alternatively as monophyletic or paraphyletic relative to the lineage leading to Ornithurae (e.g., Liu et al., 2014; Wang et al., 2020e). In particular, following the paraphyletic scenario (e.g., Wang et al., 2020e), the ancestral body plan of the ornithurine lineage including the modern birds should be interpreted as "gansuid-like" in both morphology and ecology. The definition and resolution of both diversity and phylogenetic status of the *Gansus*-like birds have thus a significant impact in the reconstruction of the evolutionary and ecological patterns which led to the emergence of the crown-birds around the mid-Cretaceous. Here, we describe an almost complete Jehol Biota euornithine. The peculiar skeletal morphology of the specimen supports its referral to a new gansuid genus and species, *Shuilingornis angelai* gen. et sp. nov.

1.1. Geological background

The Jianchang Basin is located in the eastern part of the Yanshan Fold and Thrust Belt, and along the northern margin of the North China Craton (Zhang et al., 2012; Zhu et al., 2012). The Upper Mesozoic units are nearly completely and successively distributed in this basin, in ascending order, containing the Middle Jurassic Haifanggou/Jiulongshan Formation, the Upper Jurassic Tiaojishan Formation, the Upper Jurassic-Lower Cretaceous Tuchengzi Formation, the Lower Cretaceous Yixian and Jiufotang formations. The holotype of *Shuilingornis angelai* gen. et sp. nov. was uncovered at the Lamadong locality, Jianchang County, Huludao City, Liaoning Province, China (Fig. 1). The Jiufotang Formation exposed at Lamadong locality is mainly composed of a series of yellow-green conglomerate (pebbly sandstone), grayish green tuffaceous fine sandstone, and grayish white tuffaceous siltstone, which can be subdivided into three parts and represented three sedimentary phases (Wang et al., 2020d). The fossil bird herein described was uncovered from the upper part of the Jiufotang Formation, representing shallow to moderately deep lacustrine conditions.

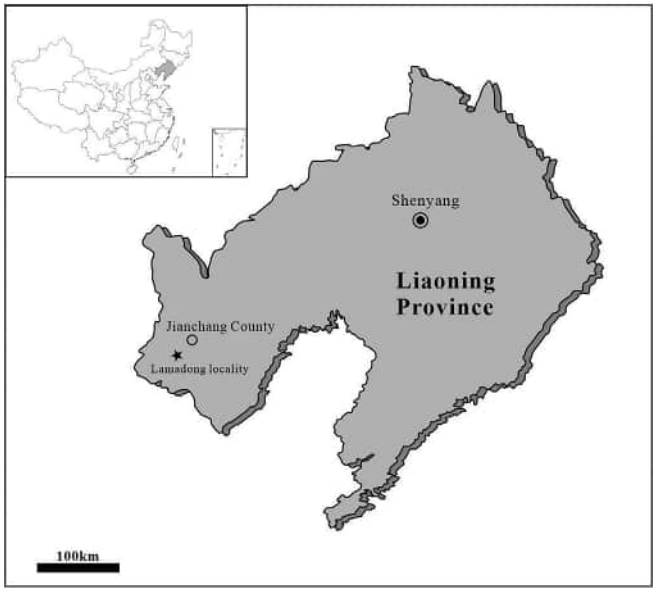

Fig. 1. Map of Liaoning Province, China, showing the Lamadong locality at Jianchang County, Huludao City, where the holotype of *Shuilingornis angelai* gen. et sp. nov. (LY2022JZ3002) was recovered.

2. Material and methods

The material described here was uncovered from the Lower Cretaceous (Aptian) Jiufotang Formation in Jianchang, Liaoning Province, China. It is a nearly complete and articulated skeleton preserved in a single slab, and is housed at Shandong Laiyang Cretaceous National Geological Park under collection number LY2022JZ3002.

We use standard sauropsid terminology for bone orientation (medial/lateral, dorsal/ventral, etc.), and apply the terms "cranial/caudal" for the postcranial skeleton instead of "anterior/posterior". The term "rostral" replace "cranial" for the description of the skull and mandible. Carpal bone homology and terminology follow the integrate paleontological and embriological framework of Botelho et al. (2014): the "*os carpi radiale*" and "*os carpi ulnare*" of Baumel and Witmer (1993) are homologus to, respectively, the scapholunare (i.e., fused radiale + intermedium) and pisiform of other sauropsids.

Following the taxonomic emendations of Benito et al. (2022), the most inclusive clade containing crown birds but excluding the enantiornithines is called "Euornithes"; the name "Ornithuromorpha" is used for the least inclusive clade containing crown birds and *Patagopteryx*.

2.1. Osteohistological analysis

The osteohistological sample was taken from the midshaft of the left ulna, and was embedded in one-component resin (EXAKT Technovit 7200) and hardened in a light polymerization device (EXAKT 520). The cross-sections were processed by sub-serially cutting the trimmed block slowly with a circular diamond saw (Isomet Buehler LTD Company) and an accurate circular saw (EXAKT 300CP). The sections were ground using the EXAKT 400CS grinding system until the desired optical contrast was obtained at a thickness of 60 μm. Successive transverse views of the bone were evaluated in transmitted light, and fluorescent light (exposure time was controlled within around 3s) using the ZEISS AX10 microscope. Images of each slice were captured using a digital camera (ZEISS AxioCam MRc5) and further processed using CorelPHOTO Paint and CorelDRAW X5 software. Histological measurements were taken from digitized cross-sections using ImageJ.

2.2. Phylogenetic analysis

We tested the affinities of *Shuilingornis* gen. nov. including a Operational Taxonomic Unit (OTU) based on LY2022JZ3002 in the phylogenetic analysis of Wang et al. (2020e) focusing on Mesozoic birds. We performed 100 "New Technology" analyses in TNT (Goloboff et al., 2008) followed by a series of "Traditional search" analyses exploring the tree islands found during the first round. The analysis found 192 shortest trees of 1692 steps each. We explored the effect of homoplastic characters on gansuid relationships performing two analyses using the "Extended Implied Weighting" function in TNT (Goloboff, 2014), setting the concavity parameter K value (which defines the downweighting of the characters according to their homoplasy) as, alternatively, 5 (an "aggressive" downweighting setting) and 15 (a "moderate" downweighting setting). The two replications using the "Extended Implied Weighting" function followed the same search protocol used in the first (equally weighted) analysis.

2.3. SEM and TEM analyses

The SEM samples were taken from the black maculae in the orbit cavity (Supplementary Fig. S1A) and abdominal area

(Supplementary Fig. S1D), respectively. Samples were placed on carbon tape on copper stubs, sputter coated with Au and examined using a JEOL JSM-6700 and a ZEISS SIGMA-500 SEM at accelerating voltages of 15–18 kV at the National Research Center for Geoanalysis in Beijing, China. The TEM sample were removed from the black macula in the abdominal area. The sampled fragment was embedded in SPI-PON 812 Resin, trimmed and cut into ultrathin sections (70 nm) using a diamond knife for the TEM and STEM imaging and element analyses, and were conducted by using a Talos F200X (FEI) at the Institute of Vertebrate Paleontology and Paleoanthropology, Chinese Academy of Sciences in Beijing, China (Supplementary Fig. S1D).

2.4. Nomenclatural act

The electronic version of this article in portable document format will represent a published work according to the International Code of Zoological Nomenclature, and hence the new names contained in the electronic version are effectively published under that Code from the electronic edition alone. This published work and the nomenclatural acts it contains have been registered in ZooBank, the online registration system for the ICZN. The ZooBank LSIDs (Life Science Identifiers) can be resolved and the associated information viewed through any standard web browser by appending the LSID to the prefix http://zoobank.org/.

This publication LSID: urn:lsid:zoobank.org:pub:286C0947-F45F-479E-9A4A-D939D47D57B7.

Genus name *Shuilingornis* gen. nov. LSID: urn:lsid:zoobank.org:act:3CBDF2C9-8DF5-431B-9579-E2DE719ECAE0.

Species name *Shuilingornis angelai* gen. et sp. nov. LSID: urn:lsid:zoobank.org:act:0A3D83CE-7333-4C76-BFEF-A7F656BEA371.

Institutional abbreviations: LY, Shandong Laiyang Cretaceous National Geological Park.

3. Systematic paleontology

Avialae Gauthier, 1986
Pygostylia Chiappe, 2002
Euornithes Sereno, 1998
Gansuidae Hou and Liu, 1984

Definition *(new)*. The most inclusive clade containing *Gansus yumenensis* but not *Hesperornis regalis, Hongshanornis longicresta*, *Patagopteryx deferrariisi*, *Songlingornis linghensis*, *Vultur gryphus* or *Yanornis martini*.

Included taxa. Based on the result of our phylogenetic analysis, Gansuidae includes the genera *Changzuiornis*, *Gansus*, *Khinganornis*, *Iteravis*, and *Shuilingornis* gen. nov. Although supported by the phylogenetic analysis, the placement in this clade of the fragmentary *Hollanda* from the Upper Cretaceous of Mongolia (Bell et al., 2010) is considered as tentative.

Diagnosis. Alveolar margin of dentary subparallel to ventral margin of bone in side view; widely spaced teeth in mid-dentary, allowing occlusal intercalation (distance among alveoli is larger than the mesiodistal diameter of alveolus); rostral margin of sternum angular, not curved; straight metacarpal III bounding a slit-like intermetacarpal space with metacarpal II; pubis distal end with prominent caudal projection; medial condyle of tibiotarsus projected more cranially than lateral condyle; tarsometatarsus longer than half tibiotarsus; distal end of metatarsal II not gynglymoid.

Shuilingornis angelai gen. et sp. nov.
(Fig. 2, Table 1)

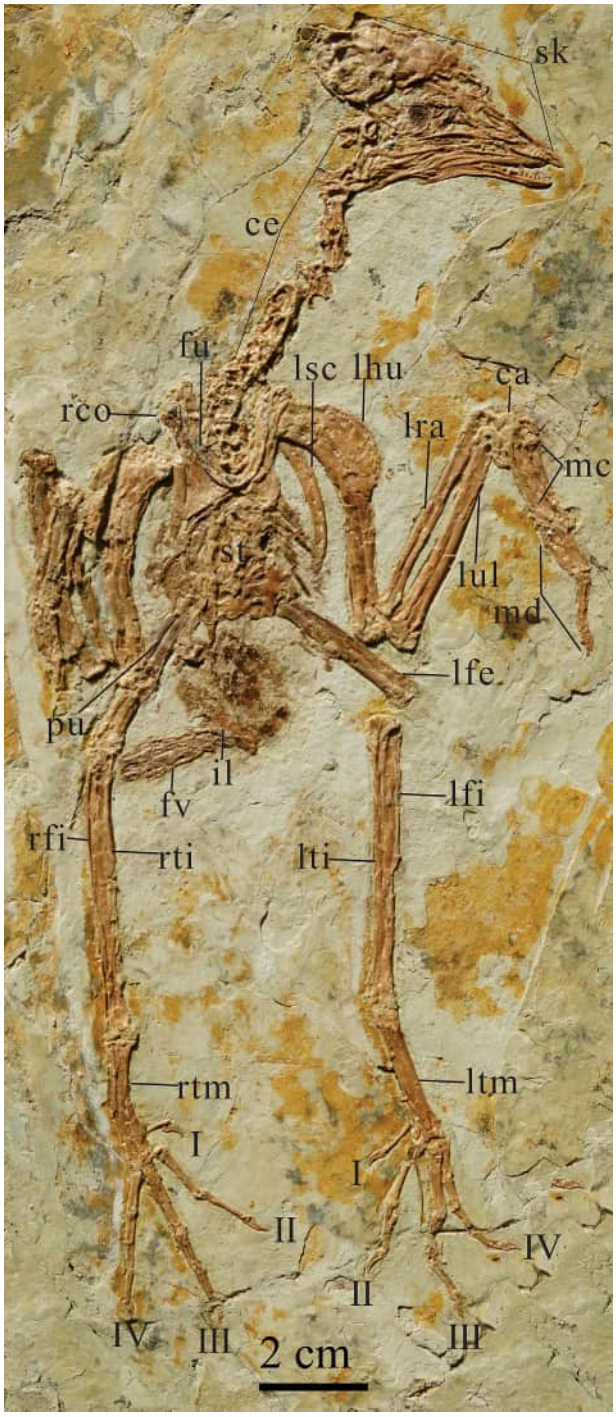

Fig. 2. Holotype of *Shuilingornis angelai* gen. et sp. nov. (LY2022JZ3002). Abbreviations: ca, carpals; ce, cervical vertebrae; fu, furcula; fv, fused vertebrae il, ilium; lfe, left femur; lfi, left fibula; lhu, left humerus; lra, left radius; lsc, left scapula; ltm, left tarsometatarsus; lul, left ulna; mc, metacarpals; md, manual digits; pu, pubis; rco, right coracoid; rfi, right fibula; rti, right tibiotarsus; rtm, right tarsometatarsus; sk, skull; st, sternum; I, II, III, IV, pedal digit I, II, III, IV. Scale bar = 2 cm.

Etymology. The genus name is composed of Chinese "*Shuiling*" ("pretty and vivid") and Greek "*ornis*" (bird). The species name honors the Italian journalist and science writer Piero Angela (1928–2022) for his extraordinary contribution to the popularization of scientific knowledge and the promotion of rational thinking.

Table 1
Measurements (in mm) of the holotype of *Shuilingornis angelai* gen. et sp. nov. (LY2022JZ3002). Abbreviations: L, left; R, right; # indicates preserved length.

Element	Length	Element	Length
Skull	47.2	Tibia	51.9 (L)
Dentary	22.8	Fibula	23.2 (L)
Furcular ramus	19.3	Metatarsal I	6.2 (L)
Coracoid	20.3 (R)	Pedal digit I–1	7.8 (L)
Scapular	27.5 (L)	Pedal digit I–2	5.0 (L)
Humerus	45.3 (L)	Metatarsal II	20.2 (L)
Ulna	41.7 (L)	Pedal digit II–1	12.0 (L)
Radius	40.5 (L)	Pedal digit II–2	9.1 (L)
Metacarpal I	5.6 (L)	Pedal digit II–3	5.6 (L)
Manual digit I–1	10.8 (L)	Metatarsal III	24.8 (L)
Manual digit I–2	7.0 (L)	Pedal digit III–1	10.3 (L)
Metacarpal II	21.1 (L)	Pedal digit III–2	8.2 (L)
Manual digit II–1	10.5 (L)	Pedal digit III–3	7.9 (L)
Manual digit II–2	10.4 (L)	Pedal digit III–4	5.1 (L)
Manual digit II–3	6.6 (L)	Metatarsal IV	20.4 (L)
Metacarpal III	21.1 (L)	Pedal digit IV–1	7.6 (L)
Manual digit III–1	6.5 (L)	Pedal digit IV–2	5.8 (L)
Fused vertebrae	21.8#	Pedal digitIV–3	4.8 (L)
Ilium	19.8	Pedal digit IV–4	6.2 (L)
Femur	30.2# (L)	Pedal digit IV–5	4.4 (L)

Holotype. LY2022JZ3002, a nearly complete and articulated skeleton preserved in a single slab (Fig. 2) and housed at Shandong Laiyang Cretaceous National Geological Park.

Locality and horizon. Lamadong locality, Jianchang County, Huludao City, Liaoning Province, China; Jiufotang Formation, Lower Cretaceous (Aptian) (Yu et al., 2021).

Diagnosis. Small euornithine bird with the unique combination of characteristics that can be distinguished from other Mesozoic birds: acuminate edentulous premaxilla longer than preantorbital ramus of maxilla; nasal with large subnarial process; procumbent maxillary teeth restricted to rostral end of bone which are much larger than the underlying dentary teeth (autapomorphy); humerus with robust shaft and elongate and gently curved deltopectoral crest; gracile alular digit less than half radius shaft width; large "U-shaped" furcula contacts the triangular apex of sternum; laterodistal end of coracoid does not define a distinct process, describing an acuminate 45° corner; manual phalangeal formula 2-3-2, with first phalanx of minor digit more than four times longer than the second phalanx.

Description and comparison. The skull is preserved in right lateral view (Fig. 3). The preorbital region occupies nearly half the skull length, similar to the condition in the non-ornithurine *Yixianornis*, *Jianchangornis* and *Khinganornis* (Zhou and Zhang, 2001; Clarke et al., 2006; Zhou et al., 2009; Wang et al., 2020e), but much shorter than in *Xinghaiornis*, *Iteravis*, *Dingavis* and *Changzuiornis* (Wang et al., 2013; Zhou et al., 2014; O'Connor et al., 2015, 2016; Huang et al., 2016). The premaxilla is tapered rostrally, with a nearly straight ventral margin and gently expanded dorsal margin. The nasal process of the premaxilla is nearly twice the length of the maxillary process and connected with the nasal. The nasal process is flattened dorsoventrally, describing a sharp medial narial shelf. As in most euornithines, the premaxilla is edentulous, different from the toothed premaxilla in the gansuid *Khinganornis* and in Yanornithidae (Wang et al., 2020a; Wang et al., 2020e). Although the maxillae are partially overlapped to determine the exact morphology, the rostral ramus appears relatively more shallow and slender than in the gansuid *Iteravis* (Zhou et al., 2014; Ju et al., 2021). Two conical teeth are preserved on the right maxilla, which are slightly expanded at the base and get sharp towards the tips. Both teeth are procumbent. There is a prominent constriction between the root and crown of the maxillary teeth. The nasal is strap-like, with a short slim premaxillary process and a wide maxillary (subnarial) process. The frontal and parietal were both dislocated dorsally during the fossilization process. The frontal is domed ventrally, with the strongly expanded caudal half much wider than the rostral half. The parietal is roughly hemispherical in lateral view, with a flat thickened dorsal margin. The jugal is long and rod-like, and rostrally articulated to the maxilla. No postorbital process of the jugal can be observed, as in other euornithines. A small triangular bone preserved between the rostral end of the two dentaries is likely the mentomeckelian (predentary), as in other euornithines but differing from *Iteravis*. The dentary is tapered rostrodorsally and expanded caudally from the middle part. The ventral margin of the dentary is gently curved dorsally, different from the straight ventral margin in the non-ornithurine *Jianchangornis* (Zhou et al., 2009). At least 13 small conical teeth are tightly packed on the left dentary, which are similar to the maxillary teeth in morphology but significantly smaller in size. Only 6 teeth can be observed on the right dentary, which are arranged sparsely. The tooth morphology is similar to that in *Yixianornis* and *Jianchangornis*, different from the elongate, distally recurved dentition in some gansuids like *Iteravis* and in hongshanornithids (Zhou and Zhang, 2001; Clarke et al., 2006; Zhou et al., 2009; Chiappe et al., 2014; Zhou et al., 2014; Liu et al., 2014). The orbital

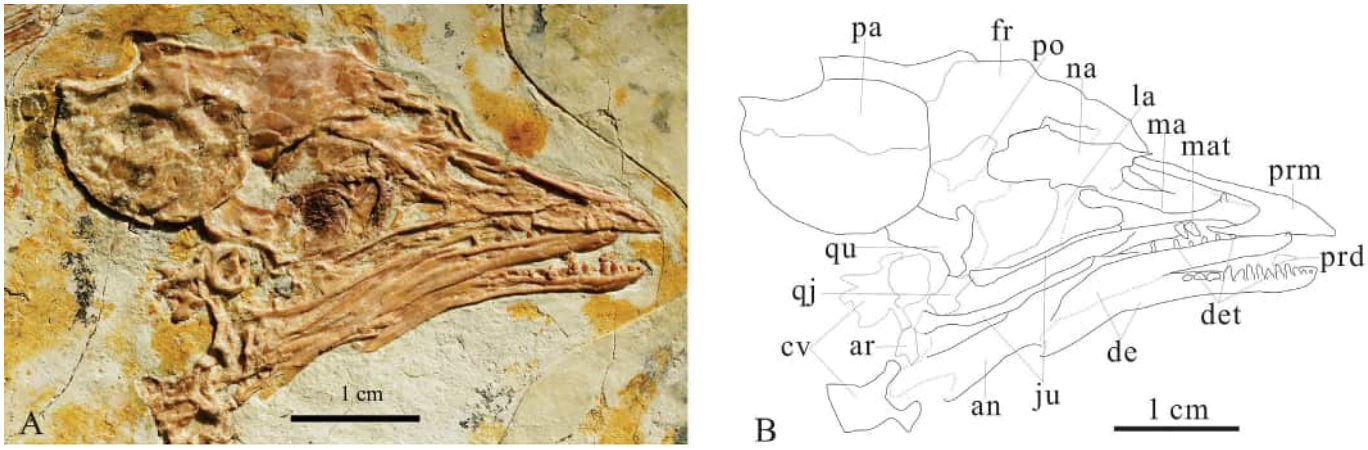

Fig. 3. Photo (A) and line drawing (B) of skull of *Shuilingornis angelai* gen. et sp. nov. (LY2022JZ3002). Abbreviations: an, angular; ar, articula; cv, cervical vertebrae; de, dentary; det, dentary teeth; fr, frontal; ju, jugal; la, lacrimal; ma, maxilla; mat, maxillary teeth; na, nasal; pa, parietal; po, postorbital; prd, predentary; prm, premaxilla; qj, quadjugal; qu, quadrate. Scale bar = 2 cm.

and postorbital areas are badly preserved. A distinct black macula is preserved inside the orbital cavity, which we interpret as remnant of the eye soft tissue.

Eleven cervical vertebrae are preserved, including the atlas and axis (Fig. 4). The atlas is round in cranial view and articulated with the square-like axis. The third cervical vertebra is also square-shaped, with a strong ventral keel. The centra of the other cervical vertebrae are more elongated craniocaudally, with prominent pre- and postzygopophyses. The preserved cervical ribs are short and do not reach the middle of the corresponding centrum. Only three dorsal vertebrae can be observed, which are larger than the cervical vertebrae and are associated to long ribs. A series of fused vertebrae is separately preserved next to the right femur (Fig. 5), but it is unclear if it represents the sacrum or the pygostyle due to the bad preservation.

The sternum is not well preserved due to the overlapping by other bones (Fig. 5). The outline is rectangular as in typical euornithines. The rostral end of the sternum describes a broad triangle fitting between the two coracoids, as in other gansuids (e.g., Liu et al., 2014), yet, it recalls the enantiornithines and some non-avian theropods in being in contact with the hypocleideal end of the furcular body (Cau et al., 2021). A small zyphoid process is visible distally and several sternal ribs are exposed laterally. The proximal end of the left scapula is overlapped by the left humerus. The exposed scapula shaft is slender and short, approximately 61% the length of the humerus, which differs from the relatively longer scapula (nearly equal to the humerus) in *Yixianornis* (Clarke et al., 2006). The scapular blade is recurved and tapered distally. The coracoid is strut-like, with a straight sternal margin. The lateral margin is straight in the proximal half and curved distally, describing an acuminate corner with the sternal facet. The furcula is more robust than in other gansuids (e.g., Liu et al., 2014). As in most euornithines, it is "U"-shaped lacking a distinct hypocleidum, with a smoothly curved sternal margin different from the straight sternal margin of *Yixianornis* (Clarke et al., 2006). The furcular rami are slightly tapered proximally and describe an interclavicular angle of about 45–50°, a value intermediate between those in other gansuids (Liu et al., 2014).

The right humerus is badly preserved, whereas the left humerus is preserved without distortion. The humerus is slightly longer than both ulna and radius, a condition opposite to that in *Jianchangornis* (Zhou et al., 2009). The humeral head is rectangular in side view, different from the elliptical to globose shape in *Yixianornis* and in many ornithuromorphs (Zhou and Zhang, 2001; Clarke et al., 2006). The deltopectoral crest is elliptical and extends more than one-third of the total humerus length. The distal half of the humeral shaft is straight, different from the laterally curved distal end in *Yixianornis* (Zhou and Zhang, 2001; Clarke et al., 2006). The ulna and radius are straight and approximately equal in length. The ulna is nearly 120 % the width of the radius. The proximal and distal ends are too badly preserved for determining the significant features. The pisiform, scapholunare and semilunate carpal are similar in size and not fused with the metacarpals (Fig. 6). The pisiform ("*os carpi ulnare*" *sensu* Baumel and Witmer, 1993) is roughly triangular and lacks the distinct dorsal and lateral processes separated by a deep incisure which are developed among the ornithurines (e.g., *Meleagris*, Baumel and Witmer, 1993; *Iaceornis*, Clarke, 2004).

Metacarpal I (alular metacarpal) is not fused with metacarpal II (major metacarpal) and metacarpal III (minor metacarpal) (Fig. 6), different from the completely fused carpometacarpus in many euornithines (e.g., *Khinganornis*, *Yixianornis*; Zhou and Zhang, 2001; Clarke et al., 2006; Wang et al., 2020e). Metacarpal I is extremely short, about 26 % the length of metacarpal II and metacarpal III. Metacarpal II is fused with metacarpal III both proximally and distally (in *Jianchangornis*, the two metacarpals are unfused, Zhou et al., 2009), but separated along the middle shaft by a narrow slit, as usual among gansuids (e.g., Liu et al., 2014). Metacarpal II is the most robust metacarpal. This differs from *Jianchangornis* which is reported to have metacarpal I being the widest and most robust metacarpal (Zhou et al., 2009). As in most euornithines, metacarpal III is as long as metacarpal II, but only half the width of the latter. Phalanx I-1 is as long as phalanx II-1 and II-2. Ungual phalanx I-2 is approximately equal in length to ungual phalanx II-3. Manual digit I is relatively short, does not extend beyond the distal end of metacarpal II, as in *Yixianornis* (Zhou and Zhang, 2001; Clarke et al., 2006), differing from *Jianchangornis* where manual digit I extends past distal end of metacarpal II (Zhou et al., 2009). The imprint of the alular feathers is partially preserved adjacent to the margin of manual digit I. Phalanx II-1 is expanded lateromedially as in most euornithines, and bears a low but distinct *pila obliqua* of trapezoid shape. Phalanx II-3 is robust, curved and sharp. Phalanx III-1 is gracile and slender, about five times longer than wide at mid-shaft.

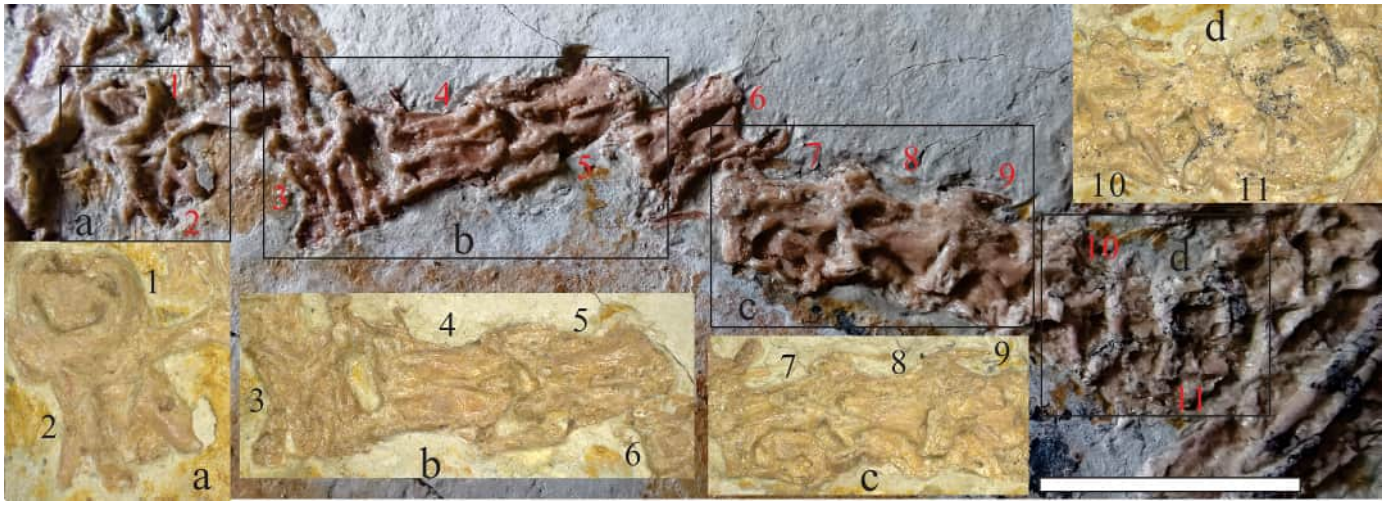

Fig. 4. Photo of cervical vertebrae of *Shuilingornis angelai* gen. et sp. nov. (LY2022JZ3002). a, the atlas and axis; b, the third to fifth cervical vertebrae; c, the seventh to ninth cervical vertebrae; d, the tenth and eleventh cervical vertebrae. Scale bar = 1 cm.

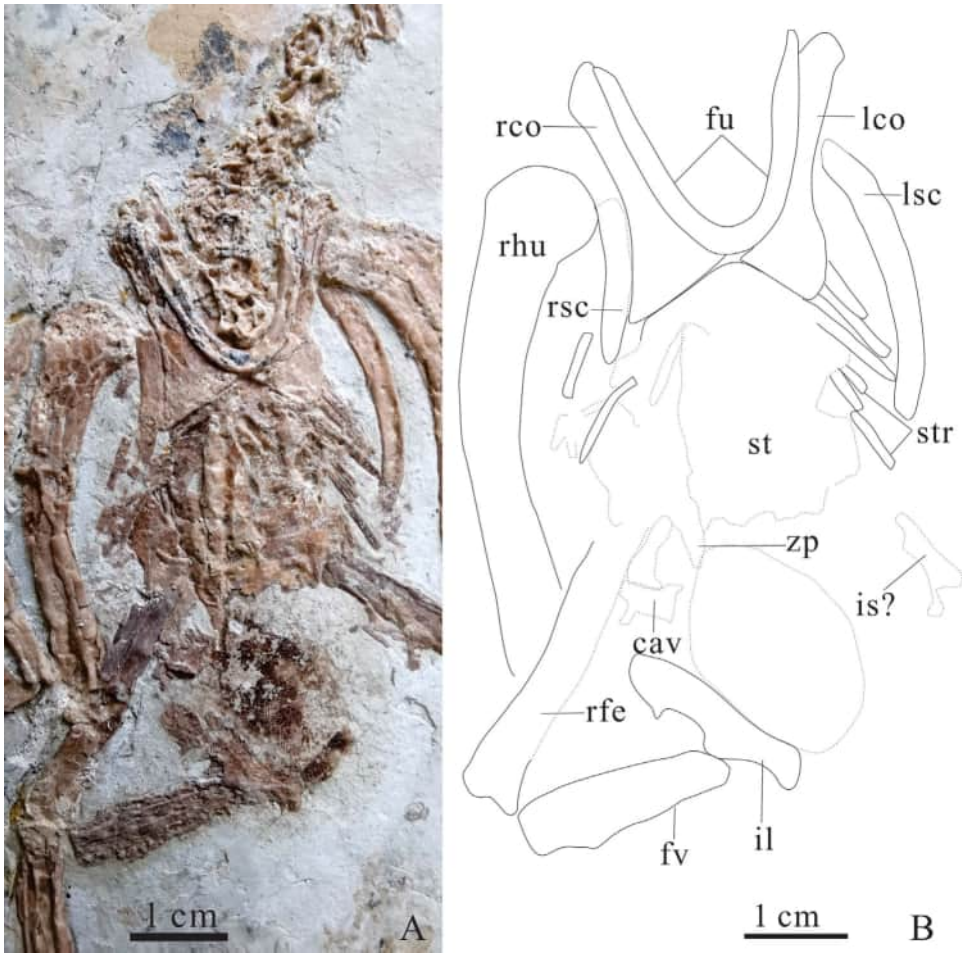

Fig. 5. Photo (A) and line drawing (B) of thoracic girdle, sternum and pelvic girdle of *Shuilingornis angelai* gen. et sp. nov. (LY2022JZ3002). Abbreviations: cav, caudal vertebrae; is?, ischium?; str, sternal ribs; zp, zyphoid process; other abbreviations as in Fig. 1. Scale bar = 1 cm.

Phalanx III-2 is extremely reduced in length (less than one fourth than the preceding phalanx) and wedge-shaped. Manual digit III differs from those of many euornithines which bear only one reduced phalanx (e.g., *Yixianornis*; Zhou and Zhang, 2001; Clarke et al., 2006). Yet, the exact phalangeal formula of the minor digit in most pygostylians is uncertain due to taphonomic issues (e.g., in *Jianchangornis*, the third finger is disarticulated and only one claw-like phalanx is visible; Zhou et al., 2009).

The pelvic bones are disarticulated and preserved in different positions, which indicates that they were not fused together. One ilium is preserved next to the series of fused vertebrae (Fig. 5). As is usual in most avialans, the preacetabular wing is much longer than the postacetabular wing (the few exceptions, like *Yixianornis*, have the pre- and post-acetabular wings subequal in length; e.g., Clarke et al., 2006). The dorsal margin of the ilium is straight. One ischium is preserved near the middle shaft of the left femur and the other is preserved over the ilium, leaving little information due to poor preservation. A partially-preserved rod-like bone is exposed next to the proximal end of the right femur, and could be part of the pubis, although no features can be determined.

The femoral shaft is straight, 160 % the length of the tarsometatarsus, and 78 % the length of the tibiotarsus. The morphology of the proximal and distal ends of the femur is unclear due to the poor preservation. The tibiotarsus is straight. The fibular shaft is extremely slim, aligned tightly with the proximal half of the tibiotarsal shaft.

Metatarsal I is not fused with the tarsometatarsus and extends proximal to the distal end of metatarsal II (Fig. 7). The distal end of metatarsal II prominently projects laterally, similar to *Gansus* (Liu et al., 2014). Metatarsal III is slightly longer than metatarsal II and metatarsal IV. Pedal digit III is the longest and most robust pedal digit, differing from *Gansus* where the longest toe is the fourth (Wang et al., 2015b). In all toes, the first phalanx is more elongate than the distal elements, as usual among Jehol Biota euornithines (e.g., Wang et al., 2020e). All pedal unguals are similar in size and morphology: they are weakly curved ventrally, bearing a shallow flexor tubercle, and with deep collateral grooves along the whole lateral surfaces (Fig. 7).

4. Results

Osteohistological analysis. We took one histological sample from the midshaft of the left ulna (Fig. 8A). The original, rather oval outline of the ulna collapsed under the pressure of the overlying sediments during fossilization. The midshaft cortex was broken into six major blocks, some of which exhibit rupture or crushing (Fig. 8B). Both intact and damaged blocks (where appropriate) were

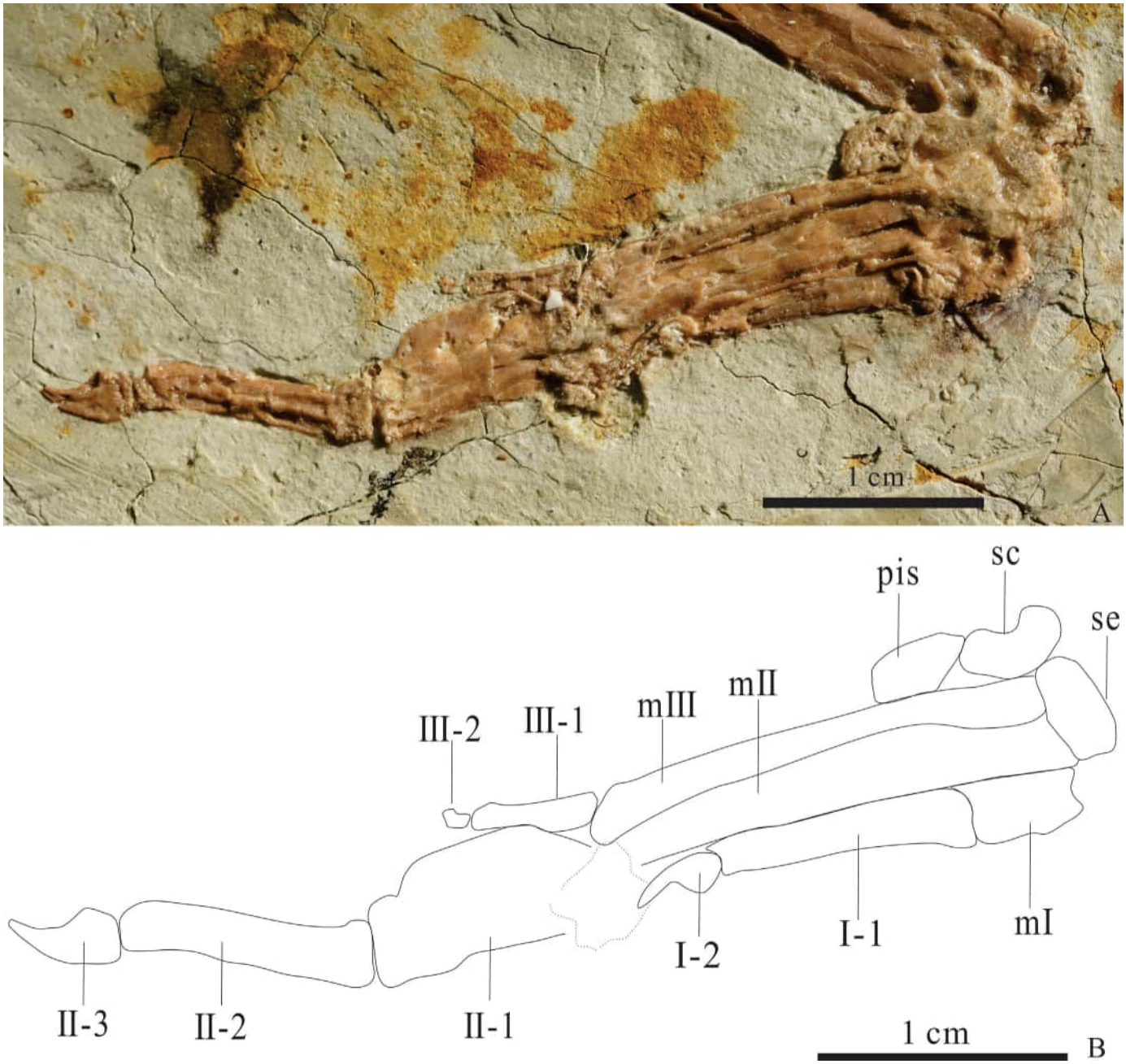

Fig. 6. Photo (A) and line drawing (B) of left hand of *Shuilingornis angelai* gen. et sp. nov. (LY2022JZ3002). Abbreviations: m I, II, III, metacarpal I, II, III; pis, pisiform; sc, scapholunare; se, semilunate carpal; I-1, 2, manual digit I-1, 2; II-1, 2, 3, manual digit II-1, 2, 3; III-1, 2, manual digit III-1, 2. Scale bar = 1 cm.

used for the description of histological microstructure, whereas, only intact blocks are used to visualize osteohistological details.

Representative histological profiles of three different sectors were selected from two successive transverse sections of the ulna midshaft; two of which are shown in transmitted light (Fig. 9A and B) and one in fluorescent light (Fig. 9C); analysis by fluorescent light allows for better recognition between osteonal and endosteal bone.

The cortex varies in thickness from 180 up to 230 μm and consists of periosteal (see the red column in Fig. 9A and B) and endosteal (see the orange column in Fig. 9A and B) bone. The periosteal bone is 140–190 μm thick, while the thickness of the endosteal (also known as the inner circumferential layer) bone varies between 30 and 50 μm; making the periosteal bone 3.5 up to 6.7 μm.

The periosteal region exhibits three different sectors when vascularity patterns are concerned. The transition from one sector to the other is not interrupted by an annulus or a line of arrested growth.

The earliest (deepest) sector (see blue column in Fig. 9) is more vascularized than all others including vascular canals projected in all three directions: laminar, longitudinal, and radial; it is usually the thickest periosteal sector ranging from 72 to 113 μm. The primary osteons are well developed and embedded into a woven bone matrix; some of the osteons, situated near the resorption line, were partly eroded (Fig. 9A).

The second (intermediate) sector (approximately 26–54 μm thick; see the green column in Fig. 9) signalizes the first significant

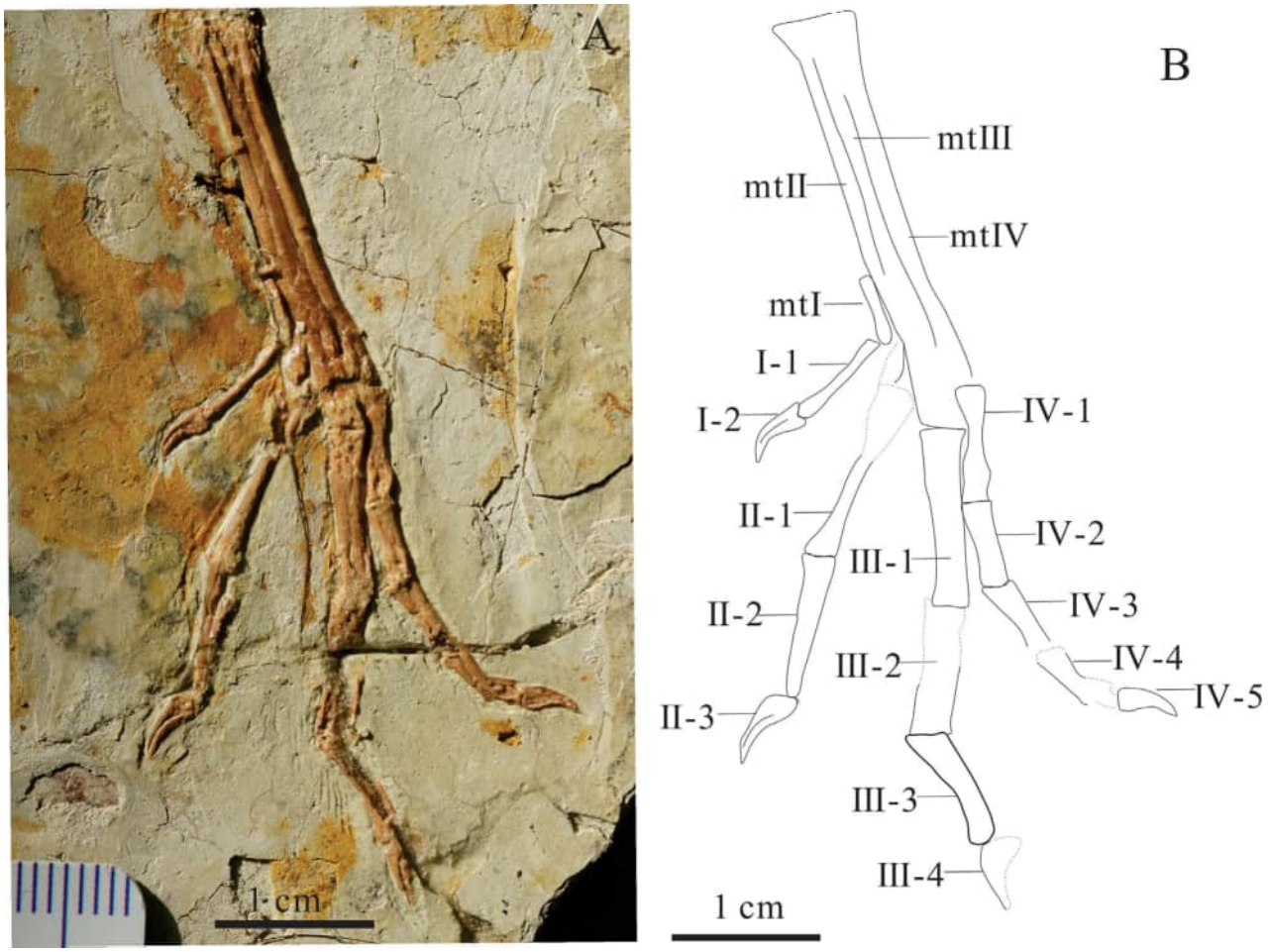

Fig. 7. Photo (A) and line drawing (B) of left foot of *Shuilingornis angelai* gen. et sp. nov. (LY2022JZ3002). Abbreviations: mt I, II, III, IV, metatarsal I, II, III, IV; I-1, 2, pedal digit I-1, 2; II-1, 2, 3, pedal digit II-1, 2, 3; III-1, 2, 3, 4, pedal digit III-1, 2, 3, 4; IV-1, 2, 3, 4, 5, pedal digit IV-1, 2, 3, 4, 5. Scale bar = 1 cm.

Fig. 8. The left ulna showing the osteohistological sample section (red arrow in A) and a complete transversal physical osteogistological section of *Shuilingornis angelai* gen. et sp. nov. (LY2022JZ3002) exhibiting collapsed cortical bone of the left ulna midshaft using transmitted light microscopy (B).

change in the formation of periosteal bone as all vascular canals are restricted to longitudinal projection and the bone matrix is more organized (compare shape [flattened], number [lower] and distribution [less random] of osteocyte lacunae in the intermediate sectors shown in Fig. 9A and B). Noteworthy, the lumina of the primary vascular canals are smaller in the second sector (e.g. from 10.1 × 5.7 μm to 14.8 × 7.7 μm) than those found in the first sector (e.g. from 22.8 × 11.7 to 26.4 × 12 μm). Another feature of the second sector is the presence of more ill-developed osteons (e.g. from 21.4 × 10.8 μm to 35.4 × 19.3 μm) in comparison with those of the first sector (e.g. 38.6 × 17.8 μm to 54.7 × 30.2 μm).

The outer margin of the intermediate sector (approximately 18–58 μm thick; see the yellow column in Fig. 9A and B) is usually characterized by the parallel-fibered bone tissue. The latest

(peripheral) sector (see the yellow column in Fig. 9) is exclusively formed by avascular parallel-fibered bone with osteocyte lacunae organized into layers (Fig. 9B).

The inner circumferential layer is well-developed and separated from the periosteal bone by an undulating resorption line (Fig. 9). This endosteal bone exhibits a variable thickness (from 29 up to 53 μm which is approximately 13–24 % of the cortex thickness) due to different rates of erosion of the earliest cortical bone depositions. Globular (and slightly flattened) osteocyte lacunae found in the inner circumferential layer indicate a relatively rapid formation of the endosteal bone. The medullary cavity of the ulna lacks trabecular structures (Fig. 9B). No remains of the medullary bone (see Bloom et al., 1941; Bailleul et al., 2019) were found in the type specimen of *Shuilingornis angelai* gen. et sp. nov.

Phylogenetic analysis. In all reconstructed shortest trees, *Shuilingornis* gen. nov. is recovered as a member of a speciose Gansuidae including the eponymous genus *Gansus* with *Iteravis*, *Khinganornis*, *Hollanda* and *Changzhuiornis*. In the analysis of Wang et al. (2020e), lacking *Shuilingornis* gen. nov., the gansuids formed a paraphyletic series leading to more crown-ward euornithines, with *Gansus* closer to ornithurines than the other *Gansus*-like forms. Gansuidae is among the most robust avialan clades reconstructed (nodal support = 4 when the fragmentary *Hollanda* is *a posteriori* pruned from calculation; Fig. 10). As in the previous versions of this data set, *Gansus*-like birds are found as more crown-ward than the *Yanornis*-like forms, but outside Ornithuromorpha (the "ornithurine + patagopterygiform" group). We tested the hypothesis that the new Jianchang specimen is an individual of *Jianchangornis* (from the same locality; Zhou et al., 2009) enforcing a sister taxon relationships between the two OTUs. When this constraint is enforced, the shortest topologies found are nine steps longer than the shortest unenforced topologies: we thus consider the referral of the new specimen to *Jianchangornis* not the best explanation of the morphological data. In particular, 17 morphological character states differentiate the two OTUs (11 optimized as autapomorphic in *Shuilingornis* gen. nov., six as autapomorphic in *Jianchangornis*), a result which dismisses the referral of the new bird to the sympatric taxon.

We explored the effect of homoplastic characters on gansuid relationships performing two analyses using the "Extended Implied Weighting" (EIW) function in TNT, setting the concavity parameter K value (which defines the downweighting of the characters according to their homoplasy) as, alternatively, 5 (an "aggressive" downweighting setting) and 15 (a "moderate" downweighting setting). The result of the first EIW analysis replicated the topology of Wang et al. (2022b), with gansuids forming a paraphyletic couple leading to Ornithuromorpha (Fig. 11A). The second EIW analysis produced a monophyletic Gansuidae as in the equally weighted analysis (Fig. 11B).

5. Discussion

The incomplete fusion of both carpometacarpus and tarsometatarsus of *Shuilingornis angelai* gen. et sp. nov. holotype might be indication of a subadult stage of somatic development at the time of death (e.g., O'Connor et al., 2015), although we cannot dismiss such features as being the retention of plesiomorphic conditions among Mesozoic birds. The preserved histology of the ulnar midshaft of *Shuilingornis* gen. nov. demonstrates a continuous growth similar to that in other Early Cretaceous euornithine taxa such as the gansuids *Iteravis* (O'Connor et al., 2015) and *Khinganornis* (Wang et al., 2020e), the avian *Vegavis* (Marsà et al., 2017), and the non-ornithuromorph *Yanornis* (Wang et al., 2020c). The presence of (P1) the inner circumferential layer, (P2) avascular parallel-fibered bone on the outer cortex, and (P3) significant histological changes between the three sectors, in combination with the absence of (A1) the lines of arrested outer, and (A2) the outer circumferential layer suggest that the specimen represents an early adult stage. It remains open to further investigation whether this advanced ontogenetic stage was reached within the first year of life as we cannot rule out at the moment that the three sectors may refer to seasonal periodicity.

Shuilingornis gen. nov. possesses several typical euornithine synapomorphies, such as the U-shaped furcula; craniocaudally elongate sternum; manus with metacarpal II and metacarpal III fused at both ends and subequal in length; a robust, craniocaudally expanded first phalanx in the second digit bearing a distinct lateral shelf and a reduced third finger. *Shuilingornis* gen. nov. is more similar to the long-legged euornithine birds (e.g., *Gansus*, *Changzuiornis*, and *Khinganornis*) by sharing the following characteristics: subparallel alveolar and ventral margins of dentary; angular rostral margin of sternum; a slit-like intermetacarpal space between metacarpal II and metacarpal III; pubis distal end with prominent caudal projection; medial condyle of tibiotarsus projected more cranially than lateral condyle; tarsometatarsus longer than half tibiotarsus; distal end of metatarsal II not gynglymoid. The phylogenetic analysis provides robust support for the monophyly of the gansuid clade including *Gansus*, *Changzuiornis*, *Khinganornis*, *Iteravis*, and *Shuilingornis* gen. nov. (Fig. 10).

Shuilingornis gen. nov. is distinguishable from other gansuids by possessing the following combination of features: the skull is mesorostrine (longirostrine in *Changzuiornis* and *Iteravis*); the premaxilla is edentulous (premaxillary teeth present in *Khinganornis*); the subnarial ramus of premaxilla is longer than the preantorbital ramus of maxilla (shorter in *Changzuiornis* and *Iteravis*); the lateral margin of the nasal ramus of premaxilla extends over half of rostrum (more than half of rostrum in *Changzuiornis*); the rostral ramus of maxilla is shallow and triangular (relatively deeper in *Iteravis*); the maxillary teeth are much larger than the dentary teeth (comparable in size in *Khinganornis*); the dentary possesses at least 13 tightly packed small and conical teeth (more numerous and slender dentary teeth in *Changzuiornis*); the sternal margin of the coracoid is half length of the coracoid and lacks a distinct lateral process (distinct lateral process in the coracoid of *Changzuiornis*, *Gansus* and *Iteravis*); the humeral head is rectangular-shaped in cranial view (shallower in *Iteravis*, more globose in *Gansus*); the humeral shaft is straight and robust (i.e., about five times its mid-shaft diameter) (more gracile in *Gansus* and *Khinganornis*); the radius is moderately robust (i.e., half ulnar mid-shaft width) (more gracile in *Gansus*); the intermembral index (humerus + ulna + metacarpal II/femur + tibiotarsus + metatarsal III) is approximately 0.92 (>1 in *Iteravis*); the distal end of metatarsal II does not reach levels of metatarsal III and IV distal ends and abruptly diverges medially relative to the more appressed distal ends of metatarsals III and IV (metatarsal II reaches levels of trochleae of metatarsals III or IV in *Khinganornis* and *Iteravis*, and in both, it does not markedly diverges medially); pedal digits II and IV are subequal in length and robustness (pedal digit IV longer than digit II in *Gansus*, *Khinganornis* and *Iteravis*); the four sharp pedal unguals are similar in size and morphology, which are poorly curved ventrally, lack prominent flexor tubercles, and possess deep grooves laterally (flexor tubercles prominent and distally-located in *Gansus*).

Shuilingornis gen. nov. differs from the other Jiufotang Formation euornithine found at Jianchang, *Jianchangornis microdonta* (Zhou et al., 2009), in bearing a ventrally curved dentary, in having the humerus longer than the radius, and in having a more slender alular metacarpal bearing a much shorter digit not extended beyond the metacarpus. The differences in both mandible and wing morphologies suggest both ecological and locomotory distinction between the two Jiufotang Formation euornithines from Jianchang.

The result of our phylogenetic analysis strongly supports the referral of *Shuilingornis* gen. nov. to Gansuidae, and indicates that

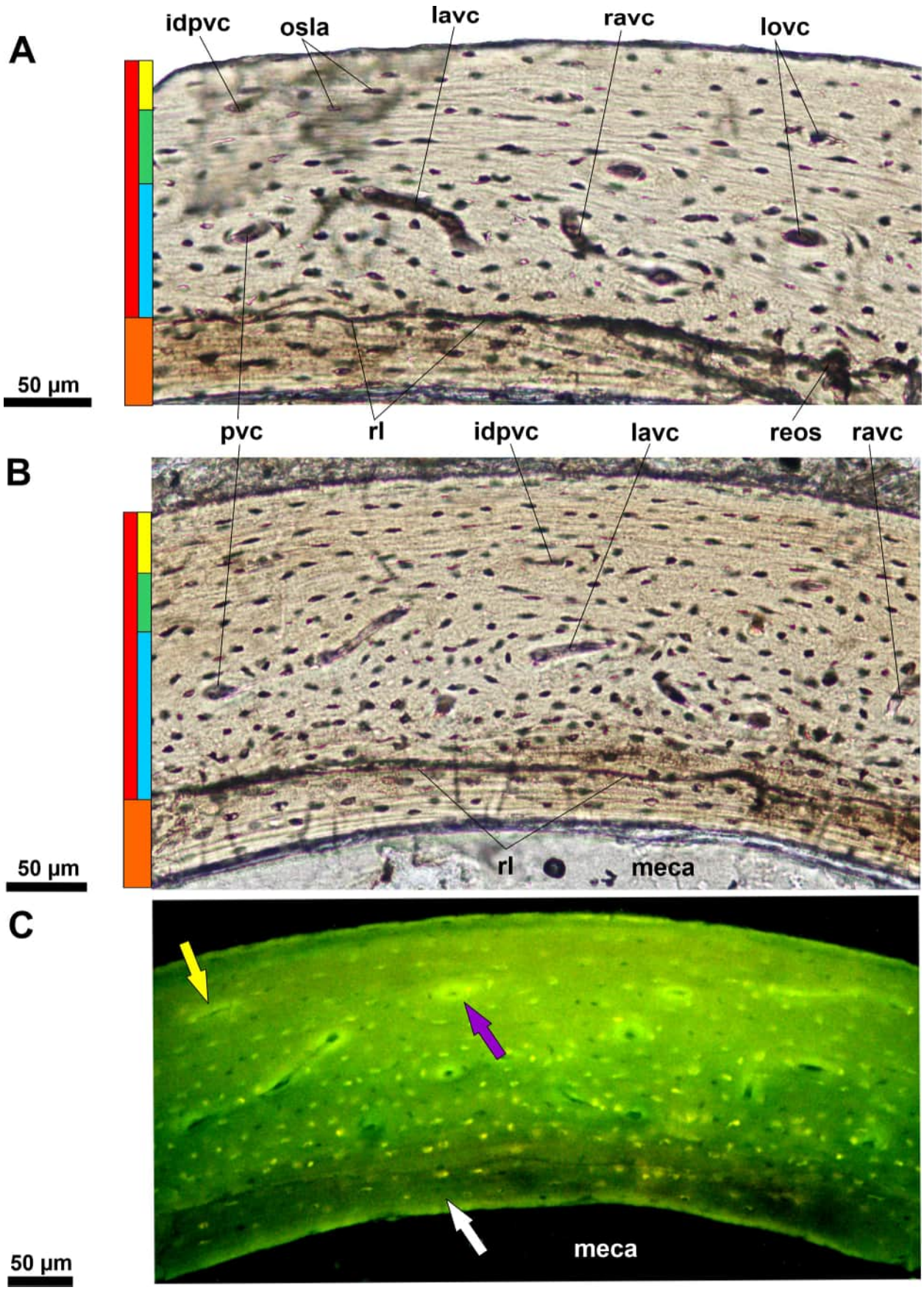
A
idpvc
osla
lavc
ravc
lovc
50 μm
B
pvc
rl
idpvc
lavc
reos
ravc
rl
meca
50 μm
C
meca
50 μm

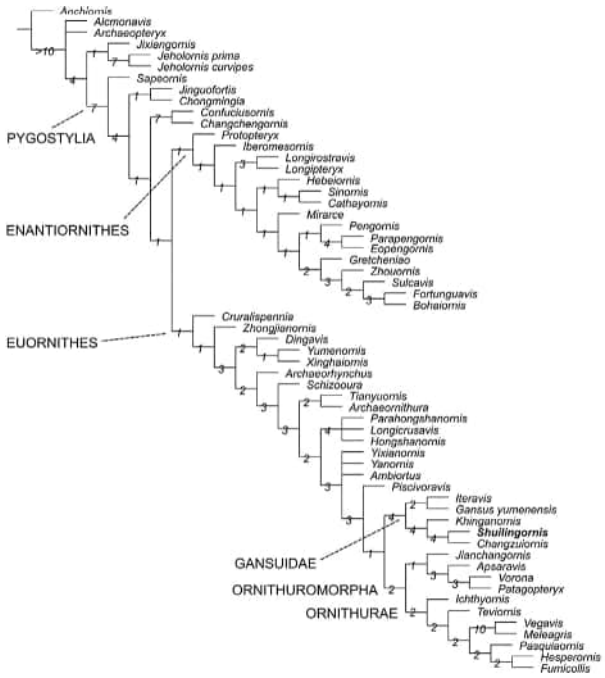

Fig. 10. Reduced strict consensus of the shortest trees reconstructed by the phylogenetic analysis. Number at nodes indicate Decay Index when four "wildcard" taxa (i.e., *Hollanda*, *Iaceornis*, *Neuquenornis*, *Qiliania*) are pruned from calculation.

this bird lineage was more diverse and speciose than previously suggested. In particular, Gansuidae includes typical "*Gansus*-like" forms, like *Iteravis* and *Khinganornis*, longirostrine taxa like *Changzuiornis*, and smaller, less specialized forms, like the new Jianchang taxon. Using the tibiotarsus as a proxy of body size, *Shuilingornis* gen. nov. is 88 % the size of *Changzuoirnis*, 80 % the size of *Khinganornis*, and 70 % the size of the largest specimens of *Gansus*. The fragmentary *Hollanda*, from the Campanian of Mongolian, might indicate the persistence of Gansuidae up to the second half of the Late Cretaceous in eastern Asia. Yet, we consider the placement of *Hollanda* in Gansuidae as provisional, pending the discovery of more complete material.

A distinct black macula is preserved inside the orbital cavity of *Shuilingornis* gen. gov. SEM analysis has been applied to ascertain whether it represents the remnant of the eye soft tissue. Unfortunately, the SEM images did not show any melanosome but resemble recent bacterial and fungine contamination of the slab or might be related to some chemical artifact occurred during fossil preparation (V. Rossi, pers. com. to AC, 2024; Supplementary Fig. S1A–C). An oval-shaped black macula is preserved inside the abdominal area (Supplementary Fig. S1D). In overall shape and position, it looks like an egg, yet no hard shell is preserved. Both SEM (Supplementary Fig. S1D–F) and TEM (Supplementary Fig. S1G–I) have been applied to analyze the structures and chemical elements. The TEM images might indicate that some mineralized soft tissue (e.g., collagen fibers) are preserved in the area defined by the "egg-like" structure.

Up to date, the gansuids have been uncovered mainly from the Changma locality, Changma Basin of northwestern China (e.g., *Gansus*, You et al., 2006; O'Connor et al., 2022), the Pigeon Hill locality, Dayangshu Basin of eastern Inner Mongolia, China (e.g., *Khinganornis*, Wang et al., 2020e), the Sihedang locality, Lingyuan Basin and the Lamadong locality, Jianchang Basin both of western Liaoning, China (e.g., *Iteravis*, *Changzuiornis* and *Shuilingornis* gen. nov., Zhou et al., 2014; Huang et al., 2016) (Fig. 12). These four basins were all formed during the middle part of the Early Cretaceous (Liu et al., 2008; Zhu et al., 2012; Kuang et al., 2013), and yielded a diversified avifauna, often dominated by euornithines (e.g., You et al., 2006) (Table 2). The holotype and referred specimens of *Gansus* were uncovered in the mudstones of the Lower Cretaceous Xiagou Formation (Hou and Liu, 1984; O'Connor et al., 2022), where the avian fossils are three-dimensionally preserved yet usually incomplete (You et al., 2006). This taphonomic pattern differs from the nearly complete preservation and articulation uncovered in the tuffaceous siltstones of the Longjiang Formation and Jiufotang Formation. From a depositional perspective, most of the gansuid-bearing layers represent freshwater bodies, with the participation of fluvio-deltaic elements in Changma (Li et al., 2020), which are consistent with the aquatic life style inferred for most gansuids (You et al., 2006). The gansuid fossil record is thus intimately linked to a combination of environmental and taphonomic conditions. The volcanic activity dramatically affected the Jehol Biota in western Liaoning and eastern Inner Mongolia, except for the Changma area, impacting both preservation and taphonomy of the delicate avian skeletons. It is remarkable that the Jehol Biota sequences in both western Liaoning and eastern Inner Mongolia were controlled by similar deep geodynamics (the subduction of the paleo-Pacific plate, Zhu et al., 2012) and record the same evolutionary intervals (the second and third phases *sensu* Li and Reisz, 2020), whereas, the Jehol Biota in Changma has been interpreted as a different paleoenvironment recording a more derived phase (Wang et al., 2015b; O'Connor et al., 2022). Avialan fossils are the dominant dinosaurian group in Changma, contrary to other Jehol Biota localities which also record bird-like (non-avialan) dinosaurs. As an example of the peculiar paleontological conditions in Changma, we focus on a monophyletic theropod lineage unique of the Jehol Biota and with a stratigraphic range similar to the gansuids, the short-armed "*Tianyuraptor*-like" dromaeosaurids (*sensu* Wang et al., 2022a): they are distributed in the other three areas but are currently absent at Changma (e.g., *Tianyuraptor* in Jianchang, *Zhenyuanlong* in Lingyuan, and *Daurlong* in eastern Inner Mongolia; Wang et al., 2022a). Non-euornithine birds, despite being present at Changma, are less abundant than the "gansuid-like" euornithines (Wang et al., 2015a). It is remarkable that Enantiornithes, the most speciose Jehol bird lineage, is widely distributed in most of the Biota, yet it represents a minority component in the gansuid-dominated units. For example, the fossil record of Bohaiornithidae ranges from northern Hebei (e.g., *Shenqiornis*, Wang et al., 2010), to Jianchang (e.g., *Bohaiornis*, Hu et al., 2011; *Sulcavis*, O'Connor et al., 2013; *Parabohaiornis*, Wang et al., 2014), and eastern Inner Mongolia (e.g., *Beiguornis*, Wang et al., 2022c). A multidisciplinary approach for interpreting the distribution of the bird lineages in the Jehol Biota is thus advocated. It should integrate the tectonic and sedimentary evolution of each basin containing the communities with a detailed analysis of the paleoclimatic and paleoenvironmental conditions.

Our analyses indicate that Gansuidae is more diverse than previously suggested. This group is remarkable in showing a series of

Fig. 9. Transversal physical sections of the left ulna midshaft of *Shuilingornis angelai* gen. et sp. nov. (LY2022JZ3002) in transmitted (A, B) and fluorescent (C) light. The cortex consists of periosteal bone (red column) and endosteal bone (orange column). Three consecutive regions are recognized in the periosteal bone with (1) diverse vascularity (blue column), (2) reduced and simplified vascularity (green column), and (3) no vascularity (yellow column). Note a high fluorescence in ill-developed (yellow arrow) and well-developed (purple arrow) primary osteons *versus* a low fluorescence of the endosteal bone of the inner circumferential layers (white arrow). Abbreviations: idpvc, ill-developed primary osteon; lavc, laminar vascular canal; lovc, longitudinal vascular canal; osla, osteocyte lacuna; meca, medullary cavity; pvc, primary vascular canal; ravc, radial vascular canal; reos, patly resorbed osteon; rl, resorption line.

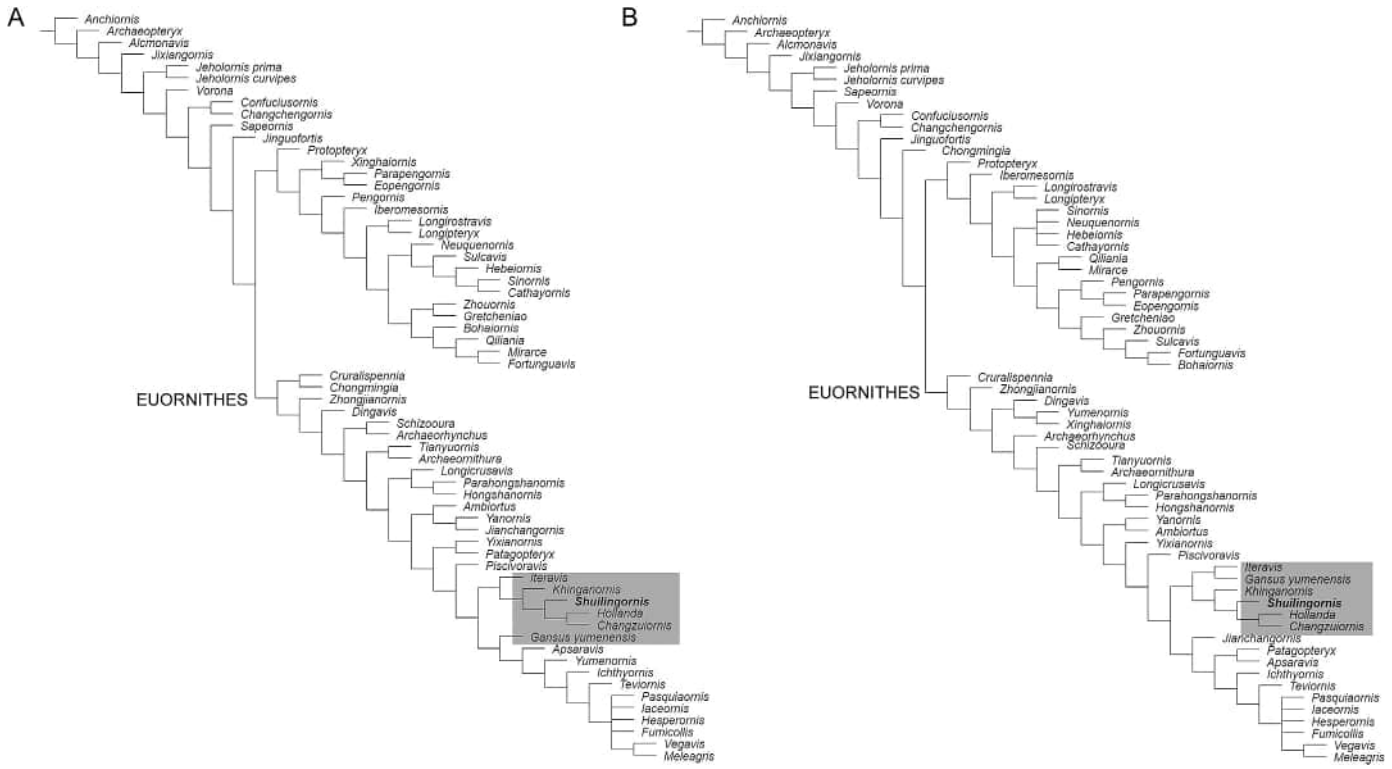

Fig. 11. Strict consensus trees of the two analyses using the "Extended Implied Weighting" function in TNT. A, analysis using $K = 5$; B, analysis using $K = 15$. Bracketed areas indicate the members of Gansuidae in the equally-weighted analysis.

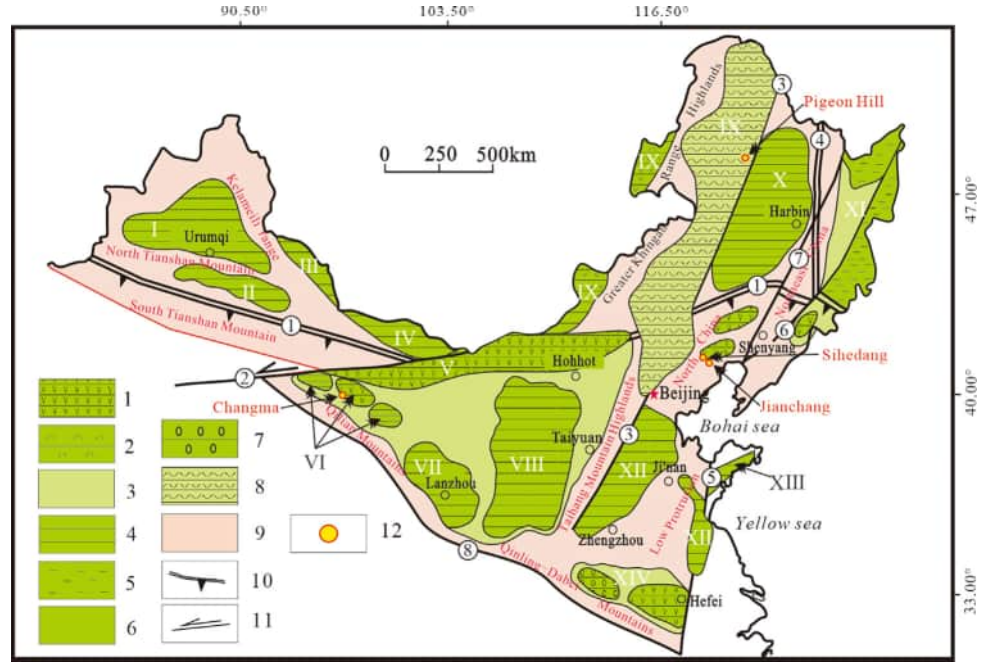

Fig. 12. Early Cretaceous paleogeography and sedimentary basin structures in North China. 1, K_1^3-K_1^2 andesite + river and lake sandstone and mudstone; 2, K_1^1 rhyolite lava + pyroclastic rock; 3, prototype basin; 4, K_1^3-K_1^2 river and lake sediments; 5, marine and continental alternative sediments; 6, relict basin; 7, K_2^1 alluvial conglomerate; 8, rhyolite lava of Zhangjiakou Formation; 9, uplift or highland, mountain range; 10, plate suture zone; 11, fault; 12, fossil localities of Gansuidae. ①, Late Paleozoic Plate Suture Zone; ②, Altyn Tagh fault; ③, Greater Khingan-Taihang Mountains Fault Zone; ④, Mudanjiang Fault Zone; ⑤, Yimu Fault Zone; ⑥, Dunmi Fault; ⑦, Yilan-Yitong Fault; ⑧, plate boundary. I, Junggar depression basin; II, Tuha depression basin; III, Santanghu fault-depression basin; IV, Beishan depression basin; V, Yin-E-Daqingshan fault basin; VI, fault basin group in the northern margin of Qilian Mountains; VII, fault basin group of Lanzhou-Minhe-Liupanshan; VIII, Ordos depression basin; IX, fault basin group in the western Khingan Mountains; X, Songliao fault basin; XI, Sanjiang fault basin group; XII, rift basin group of North China-Yishu; XIII, Jiaolai fault basin; XIV, fault basin group in the northern margin of Dabie Mountains. The Early Cretaceous is divided into three periods: K_1^1: 145~130 Ma, K_1^2: 130~120 Ma and K_1^3: 120~110 Ma. Based on Kuang et al. (2013).

Table 2
The components of avifauna in four localities, where the gansuids were recovered.

Locality	Lithostratigraphy (Lower Cretaceous)	Avifauna		
		Euornithes	Enantiornithes	Basal birds
Lamadong, Jianchang	Jiufotang Formation	*Jianchangornis microdonta; Schizooura lii; Archaeorhynchus spathula; Bellulia rectusunguis; Mengciusornis dentatus; Shuilingornis angelai* gen. et sp. nov.	*Bohaiornis guoi; Sulcavis geeorum*; *Parabohaiornis martini; Longusunguis kurochkini; Fortunguavis xiaotaizicus; Linyiornis amoena*	*Jeholornis palmapenis*
Sihedang, Lingyuan	Jiufotang Formation	*Dingavis longimaxilla; Iteravis huchzermeyeri; Changzuiornis ahgmi*; *Juehuaornis zhang*;	*Monoenantiornis sihedangia; Piscivorenantiornis inusitatus*	*Yangavis confucii*
Pigeon Hill, eastern Inner Mongolia	Longjiang Formation	*Khinganornis hulunbuirensis*	*Beiguornis khinganensis*	/
Changma, northwestern China	Xiagou Formation	*Gansus yumenensis*; *Yumenornis huangi; Jiuquanornis niui; Changmaornis houi; Meemannavis ductrix; Brevidentavis zhangi*	*Qiliania graffini; Dunhuangia cuii; Feitianius paradisi*	/

adaptations to the semi-aquatic realm paralleling the modern birds (You et al., 2006). The discovery of relatively unspecialized gansuids like *Shuilingornis* gen. nov. weakens a direct evolutionary link between the aquatic adaptations shared by Gansuidae and Ornithurae, suggesting multiple episodes of exploration of that ecomorphology among Euornithes during the Cretaceous. This interpretation dismisses the "gansuid bauplan" as ancestral to the root of the modern avians (a scenario which was implicit in some phylogenetic analyses reconstructing the gansuids as paraphyletic to the ornithuromorphs; e.g., Wang et al., 2020e). The tentative referral of the Mongolian euornithine *Hollanda* to the gansuid clade is intriguing but needs further evidence for being confirmed. Yet, it might indicate a broader geographic and stratigraphic distribution of the gansuids beyond the Jehol Biota. Different lines of evidence thus converge to the hypothesis that Gansuidae was among the most successful lineages of Cretaceous euornithines before the origin of the modern avian radiation.

6. Conclusion

In this paper, we describe and erect a new genus and species of euornithine bird, *Shuilingornis angelai* gen. et sp. nov., from the Early Cretaceous (Aptian) Jehol Biota of western Liaoning, China. The osteohistological analysis indicates that *Shuilingornis angelai* gen. et sp. nov. holotype demonstrates a continuous growth and represents an early adult stage at the time of death. Both the morphological and phylogenetic analyses support the referral of *Shuilingornis* gen. nov. to Gansuidae, which also includes the genera *Gansus*, *Changzuiornis*, *Iteravis*, and *Khinganornis*. The definition and diagnosis of Gansuidae are proposed based on the comprehensive study of the currently referred genera. *Shuilingornis* gen. nov. provides more information on understanding the morphology and osteohistology of gansuids, and indicates that this bird lineage was more diverse than previously suggested.

CRediT authorship contribution statement

Xuri Wang: Writing – review & editing, Writing – original draft, Supervision, Project administration, Investigation, Funding acquisition, Conceptualization. **Andrea Cau:** Writing – review & editing, Writing – original draft, Software, Methodology, Formal analysis, Data curation, Conceptualization. **Yinuo Wang:** Visualization, Investigation, Conceptualization. **Martin Kundrát:** Writing – original draft, Methodology, Formal analysis, Conceptualization. **Guili Zhang:** Investigation, Conceptualization. **Yichuan Liu:** Investigation, Conceptualization. **Luis M. Chiappe:** Conceptualization.

Declaration of competing interest

The authors declare that they have no known competing financial interests or personal relationships that could have appeared to influence the work reported in this paper.

Data availability

The data that has been used is confidential.

Acknowledgments

This study was supported financially by China Geological Survey (DD20230221) and National Natural Science Foundation of China (42472002) awarded to Wang X-R., and by the Scientific Grant Agency VEGA of the Ministry of Education, Science, Research and Sport of the Slovak Republic (1/0075/22) and the Slovak Research and Development Agency (APVV-21-0319) awarded to M.K. We thank V. Rossi (University College Cork, Ireland) and Z-H Li (Institute of Vertebrate Paleontology and Paleoanthropology, Chinese Academy of Sciences) for the useful suggestions on the SEM and TEM analyses performed on the specimen. We appreciate Dr. Michael Pittman and Prof. Xiaoli Wang for their constructive comments which have helped us to significantly improve the quality of our manuscript. Thanks go to Editor-in-Chief Maria Rose Petrizzo and Associate Editor Marcin Machalski of the Cretaceous Research for their comments and handling this manuscript.

References

Bailleul, A.M., O'Connor, J.K., Zhang, S., Li, Z., Wang, Q., Lamanna, M.C., Zhu, X., Zhou, Z., 2019. An Early Cretaceous enantiornithine (Aves) preserving an unlaid egg and probable medullary bone. Nature Communications 10, 1275. https://doi.org/10.1038/s41467-019-09259-x.

Baumel, J.J., Witmer, L.M., 1993. Handbook of avian anatomy: nomina anatomica avium, second ed. Publications of the Nuttall Ornithological Club, pp. 45–132.

Bell, A.K., Chiappe, L.M., Erickson, G.M., Suzuki, S., Watabe, M., Barsbold, R., Tsogtbaatar, K., 2010. Description and ecologic analysis of Hollanda luceria, a Late Cretaceous bird from the Gobi Desert (Mongolia). Cretaceous Research 31, 16–26. https://doi.org/10.1016/j.cretres.2009.09.001.

Benito, J., Chen, A., Wilson, L.E., Bhullar, B.S., Burnham, D., Field, D.J., 2022. Forty new specimens of *Ichthyornis* provide unprecedented insight into the postcranial morphology of crownward stem group birds. PeerJ 10, e13919. https://doi.org/10.7717/peerj.13919.

Bloom, W., Bloom, M.A., McLean, F.C., 1941. Calcification and ossification. Medullary bone changes in the reproductive cycle of female pigeons. The Anatomical Record 81, 443–475.
Botelho, J.F., Ossa-Fuentes, L., Soto-Acuña, S., Smith-Paredes, D., Nuñez-León, D., Salinas-Saavedra, M., Ruiz-Flores, M., Vargas, A.O., 2014. New developmental evidence clarifies the evolution of wrist bones in the dinosaur–bird transition. PLoS Biology 12, e1001957. https://doi.org/10.1371/journal.pbio.1001957.
Cau, A., 2018. The assembly of the avian body plan: a 160-million-year long process. Bollettino della Societa Paleontologica Italiana 57, 1–25.
Cau, A., Beyrand, V., Barsbold, R., Tsogtbaatar, K., Godefroit, P., 2021. Unusual pectoral apparatus in a predatory dinosaur resolves avian wishbone homology. Scientific Reports 11, 14722. https://doi.org/10.1038/s41598-021-94285-3.
Chiappe, L.M., Ji, S., Ji, Q., Norell, M.A., 1999. Anatomy and systematics of the Confuciusornithidae (Theropoda: Aves) from the Late Mesozoic of northeastern China. Bulletin of the AMNH 242, 1–89.
Chiappe, L.M., Zhao, B., O'Connor, J.K., Gao, C., Wang, X., Habib, M., Marugan-Lobon, J., Meng, Q., Cheng, X., 2014. A new specimen of the Early Cretaceous bird *Hongshanornis longicresta*: insights into the aerodynamics and diet of a basal ornithuromorph. PeerJ 2, e234. https://doi.org/10.7717/peerj.234.
Clarke, J.A., 2004. Morphology, phylogenetic taxonomy, and systematics of *Ichthyornis* and *Apatornis* (Avialae: Ornithurae). Bulletin of the AMNH 286, 1–179. https://doi.org/10.1206/0003-0090(2004)286<0001:MPTASO>2.0.CO;2.
Clarke, J.A., Zhou, Z., Zhang, F., 2006. Insight into the evolution of avian flight from a new clade of Early Cretaceous ornithurines from China and the morphology of *Yixianornis grabaui*. Journal of Anatomy 208, 287–308. https://doi.org/10.1111/j.1469-7580.2006.00534.x.
Goloboff, P.A., 2014. Extended implied weighting. Cladistics 30 (3), 260–272.
Goloboff, P.A., Farris, J.S., Nixon, K.C., 2008. TNT, a free program for phylogenetic analysis. Cladistics 24, 774e786. https://doi.org/10.1111/j.1096-0031.2008.00217.x.
Hou, L., Liu, Z., 1984. A new fossil bird from Lower Cretaceous of Gansu and early evolution of birds. Scientia Sinica, Series B 27, 1296–1301.
Hu, D., Li, L., Hou, L., Xu, X., 2011. A new enantiornithine bird from the Lower Cretaceous of western Liaoning, China. Journal of Vertebrate Paleontology 31, 154–161.
Huang, J., Wang, X., Hu, Y., Liu, J., Peteya, J.A., Clarke, J.A., 2016. A new ornithurine from the Early Cretaceous of China sheds light on the evolution of early ecological and cranial diversity in birds. PeerJ 4, e1765. https://doi.org/10.7717/peerj.1765.
Ju, S., Wang, X., Liu, Y., Wang, Y., 2021. A reassessment of *Iteravis huchzermeyeri* and *Gansus zheni* from the Jehol biota in western Liaoning, China. China Geology 4, 197–204. https://doi.org/10.31035/cg2020066.
Kuang, H., Liu, Y., Liu, Y., Peng, N., Xu, H., Dong, C., Chen, J., Liu, H., Xu, J., Xue, P., 2013. Stratigraphy and depositional palaeogeography of the Early Cretaceous basins in Da Hinggan Mountains-Mongolia orogenic belt and its neighboring areas. Geological Bulletin of China 32, 1063–1084 (in Chinese with English abstract).
Li, X., Reisz, R., 2020. The stratigraphy and paleoenvironment of a 'Lycoptera Bed' site in eastern Inner Mongolia, China: Correlation with the fossiliferous Lower Cretaceous strata in western Liaoning. Palaeogeography, Palaeoclimatology, Palaeoecology 559, 109951. https://doi.org/10.1016/j.palaeo.2020.109951.
Li, S., Wang, Q., Zhang, H., 2020. Charophytes from the Lower Cretaceous Xiagou Formation in the Jiuquan Basin (northwestern China) and their palaeogeographical significance. Cretaceous Research 105, 103940. https://doi.org/10.1016/j.cretres.2018.08.010.
Liu, Z., Wu, X., Zhu, D., Cui, M., Liu, X., Li, X., 2008. Structural features and deformation stages of the Dayangshu Basin in northeast China. Journal of Jilin University (Earth Science Edition) 38, 27–33 (in Chinese with English abstract).
Liu, D., Chiappe, L.M., Zhang, Y., Bell, A., Meng, Q., Ji, Q., Wang, X., 2014. An advanced, new long-legged bird from the Early Cretaceous of the Jehol Group (northeastern China): insights into the temporal divergence of modern birds. Zootaxa 3884, 253–266. https://doi.org/10.11646/zootaxa.3884.3.4.
Marsà, J.A.G., Agnolín, F.L., Novas, F., 2017. Bone microstructure of *Vegavis iaai* (Aves, Anseriformes) from the Upper Cretaceous of Vega Island, Antarctic Peninsula. Historical Biology 31, 163–167. https://doi.org/10.1080/08912963.2017.1348503.
O'Connor, J.K., Zhou, Z., 2012. A redescription of *Chaoyangia beishanensis* (Aves) and a comprehensive phylogeny of Mesozoic birds. Journal of Systematic Palaeontology 11, 889–906. https://doi.org/10.1080/14772019.2012.690455.
O'Connor, J.K., Gao, K., Chiappe, L.M., 2010. A new ornithuromorph (Aves: Ornithothoraces) bird from the Jehol Group indicative of higher-level diversity. Journal of Vertebrate Paleontology 30, 311–321. https://doi.org/10.1080/02724631003617498.
O'Connor, J.K., Zhang, Y., Chiappe, L.M., Meng, Q., Li, Q., Liu, D., 2013. A new enantiornithine from the Yixian Formation with the first recognized avian enamel specialization. Journal of Vertebrate Paleontology 33, 1–12. https://doi.org/10.1080/02724634.2012.719176.
O'Connor, J.K., Wang, M., Zhou, S., Zhou, Z., 2015. Osteohistology of the Lower Cretaceous Yixian Formation ornithuromorph (Aves) *Iteravis huchzermeyeri*. Palaeontologia Electronica 18 (2), 1–11. https://doi.org/10.26879/520, 35A.
O'Connor, J.K., Wang, M., Hu, H., 2016. A new ornithuromorph (Aves) with an elongate rostrum from the Jehol Biota, and the early evolution of rostralization in birds. Journal of Systematic Palaeontology 14, 939–948. https://doi.org/10.1080/14772019.2015.1129518.
O'Connor, J.K., Stidham, T.A., Harris, J.D., Lamanna, M.C., Bailleul, A.M., Hu, H., Wang, M., You, H., 2022. Avian skulls represent a diverse ornithuromorph fauna from the Lower Cretaceous Xiagou Formation, Gansu Province, China. Journal of Systematics and Evolution 60, 1172–1198. https://doi.org/10.1111/jse.12823.
Wang, X.R., O'Connor, J.K., Zhao, B., Chiappe, L.M., Gao, C., Cheng, X., 2010. New species of Enantiornithes (Aves: Ornithothoraces) from the Qiaotou Formation in northern Hebei, China. Acta Geologica Sinica 84, 247–256.
Wang, X.R., Chiappe, L.M., Teng, F., Ji, Q., 2013. *Xinghaiornis lini* (Aves: Ornithothoraces) from the Early Cretaceous of Liaoning: an example of evolutionary mosaic in early birds. Acta Geologica Sinica 87, 686–689. https://doi.org/10.1111/1755-6724.12080.
Wang, M., Zhou, Z., O'Connor, J.K., Zelenkov, N.V., 2014. A new diverse enantiornithine family (Bohaiornithidae fam. nov.) from the Lower Cretaceous of China with information from two new species. Vertebrata PalAsiatica 52, 31–76.
Wang, M., Li, D., O'Connor, J.K., Zhou, Z., You, H., 2015a. Second species of enantiornithine bird from the Lower Cretaceous Changma Basin, northwestern China with implications for the taxonomic diversity of the Changma avifauna. Cretaceous Research 55, 56–65.
Wang, Y.M., O'Connor, J.K., Li, D., You, H., 2015b. New information on postcranial skeleton of the Early Cretaceous *Gansus yumenensis* (Aves: Ornithuromorpha). Historical Biology 28, 666–679. https://doi.org/10.1080/08912963.2015.1006217.
Wang, M., Li, Z., Zhou, Z., 2017. Insight into the growth pattern and bone fusion of basal birds from an Early Cretaceous enantiornithine bird. PNAS 114, 11470–11475. https://doi.org/10.1073/pnas.1707237114.
Wang, M., Li, Z., Liu, Q., Zhou, Z., 2020a. Two new Early Cretaceous ornithuromorph birds provide insights into the taxonomy and divergence of Yanornithidae (Aves: Ornithothoraces). Journal of Systematic Palaeontology 18, 1805–1827.
Wang, M., O'Connor, J.K., Bailleul, A.M., Li, Z., 2020b. Evolution and distribution of medullary bone: evidence from a new Early Cretaceous enantiornithine bird. National Science Review 7, 1068–1078. https://doi.org/10.1093/nsr/nwz214.
Wang, J.Y., Hao, X., Kundrát, M., Liu, Z., Uesugi, K., Jurašeková, Z., Guo, B., Hoshino, M., Li, Y., Monfroy, Q., Zhou, B., Fabriela, G., Kang, A., Wang, M., Si, Y., Gao, J., Xu, G., Li, Z., 2020c. Bone tissue histology of the Early Cretaceous bird *Yanornis*: evidence for a diphyletic origin of modern avian growth strategies within Ornithuromorpha. Historical Biology 32, 1422–1434. https://doi.org/10.1080/08912963.2019.1593405.
Wang, S.M., Zang, D., Wang, X., Li, J., Han, S., Li, J., 2020d. Oil shale features and Sedimentary environment in Jianchang Basin, Western Liaoning Province. Journal of Jilin University (Earth Science Edition) 50, 326–340 (in Chinese with English abstract).
Wang, X.R., Cau, A., Kundrát, M., Chiappe, L.M., Ji, Q., Wang, Y., Li, T., Wu, W., 2020e. A new advanced ornithuromorph bird from Inner Mongolia documents the northernmost geographic distribution of the Jehol paleornithofauna in China. Historical Biology 33, 1705–1717. https://doi.org/10.1080/08912963.2020.1731805.
Wang, X.R., Cau, A., Guo, B., Ma, F., Qing, G., Liu, Y., 2022a. Intestinal preservation in a birdlike dinosaur supports conservatism in digestive canal evolution among theropods. Scientific Reports 12, 19965. https://doi.org/10.1038/s41598-022-24602-x.
Wang, X.R., Cau, A., Luo, X., Kundrát, M., Wu, W., Ju, S., Guo, Z., Liu, Y., Ji, Q., 2022b. A new bohaiornithid-like bird from the Lower Cretaceous of China fills a gap in enantiornithine disparity. Journal of Paleontology 96, 961e976. https://doi.org/10.1017/jpa.2022.12.
Wang, X.R., Ju, S., Wu, W., Liu, Y., Guo, Z., Ji, Q., 2022c. The first enantiornithine bird from the Lower Cretaceous Longjiang Formation in the Great Khingan Range of Inner Mongolia. Acta Geologica Sinica 96, 337e348 (in Chinese with English abstract).
Wang, X.L., Clark, A.D., O'Connor, J.K., Zhang, X., Wang, X., Zheng, X., Zhou, Z., 2024. First Edentulous Enantiornithine (Aves: Ornithothoraces) from the Lower Cretaceous Jehol Avifauna. Cretaceous Research 159, 105867. https://doi.org/10.1016/j.cretres.2024.105867.
Wu, Y., Ge, Y., Hu, H., Stidham, T.A., Li, Z., Bailleul, A.M., Zhou, Z., 2023. Intra-gastric phytoliths provide evidence for folivory in basal avialans of the Early Cretaceous Jehol Biota. Nature Communications 14, 4558. https://doi.org/10.1038/s41467-023-40311-z.
Yu, Z., Wang, M., Li, Y., Deng, C., He, H., 2021. New geochronological constraints for the Lower Cretaceous Jiufotang Formation in Jianchang Basin, NE China, and their implications for the late Jehol Biota. Palaeogeography, Palaeoclimatology, Palaeoecology 583, 110657. https://doi.org/10.1016/j.palaeo.2021.110657.
You, H., Lamanna, M.C., Harris, J.D., Chiappe, L.M., O'Connor, J.K., Ji, S., Lu, J., Yuan, C., Li, D., Zhang, X., Lacovara, K.J., Dodson, P., Ji, Q., 2006. A nearly modern amphibious bird from the Early Cretaceous of Northwestern China. Science 312, 1640–1643. https://doi.org/10.1126/science.1126377.
Zhang, L., Zhang, L., Yang, Y., Guo, S., Wang, W., Zheng, Y., Ding, Q., Cheng, L., 2012. Division of the Lower Cretaceous Yixian Formation and its ostracod fossils in Jianchang Basin, western Liaoning. Geology and Resources 21, 81–92 (in Chinese with English abstract).
Zheng, X., O'Connor, J.K., Wang, X., Wang, Y., Zhou, Z., 2018. Reinterpretation of a previously described Jehol bird clarifies early trophic evolution in the Ornithuromorpha. Proceedings of the Royal Society B 285, 20172494. https://doi.org/10.1098/rspb.2017.2494.
Zhou, Z.H., 2004. The origin and early evolution of birds: discoveries, disputes, and perspectives from fossil evidence. Naturwissenschaften 91, 455–471. https://doi.org/10.1007/s00114-004-0570-4.

Zhou, Z.H., 2014. The Jehol Biota, an Early Cretaceous terrestrial Lagerstätte: new discoveries and implications. National Science Review 1, 543–559. https://doi.org/10.1093/nsr/nwu055.
Zhou, Z.H., Zhang, F., 2001. Two new ornithurine birds from the Early Cretaceous of western Liaoning, China. Chinese Science Bulletin 46, 1258–1264. https://doi.org/10.1007/BF03184320.
Zhou, Z.H., Zhang, F., 2002. A long-tailed, seed-eating bird from the Early Cretaceous of China. Nature 418, 405–409. https://doi.org/10.1038/nature00930.
Zhou, Z.H., Wang, M., 2024. Cretaceous fossil birds from China. Geological Society, London, Special Publications 544. https://doi.org/10.1144/SP544-2023-129. SP544-2023-129.
Zhou, Z.H., Zhang, F., Li, Z., 2009. A new basal ornithurine bird (*Jianchangornis microdonta* gen. et sp. nov.) from the Lower Cretaceous of China. Vertebrata PalAsiatica 47, 299–310.
Zhou, S., O'Connor, J.K., Wang, M., 2014. A new species from an ornithuromorph (Aves: Ornithothoraces) dominated locality of the Jehol Biota. Chinese Science Bulletin 59, 5366–5378. https://doi.org/10.1007/s11434-014-0669-8.
Zhu, R., Xu, Y., Zhu, G., Zhang, H., Xia, Q., Zheng, T., 2012. Destruction of the North China craton. Science China Earth Sciences 55, 1565–1587. https://doi.org/10.1007/s11430-012-4516-y.

Appendix A. Supplementary data

Supplementary data to this article can be found online at https://doi.org/10.1016/j.cretres.2024.106014.